

INITIAL STATE PARTON BROADENING AND ENERGY LOSS PROBED IN $d + Au$ AT RHIC

Ivan Vitev*

Iowa State University, Department of Physics and Astronomy

Ames, IA 50010, USA

(Dated: November 6, 2018)

Abstract

The impact parameter and rapidity dependence of the Cronin effect for massless pions in $d + Au$ reactions at $\sqrt{s_{NN}} = 200$ GeV at RHIC is computed in the framework of pQCD multiple elastic scattering on a nuclear target. We introduce a formalism to incorporate initial state energy loss in perturbative calculations and take into account the elastic energy loss in addition to the transverse momentum broadening of partons. We argue that the centrality dependence of the Cronin effect can distinguish between different hadron production scenarios at RHIC. Its magnitude and rapidity dependence are shown to carry important experimental information about the properties of cold nuclear matter up to the moderate- and large- x antishadowing/EMC regions.

PACS numbers: 12.38.Mh; 24.85.+p; 25.75.-q

*Electronic address: ivitev@iastate.edu

I. INTRODUCTION

The discovery of jet quenching [1, 2] at RHIC and its derivative signatures - the high- p_T azimuthal asymmetry [3] and the disappearance of back-to-back correlations [4] - are among the most direct evidence for the creation of dense QCD matter in nucleus-nucleus collisions. Recent theoretical work [5, 6] has provided successful qualitative and quantitative explanation of the experimental data via the techniques of perturbative QCD with strong partonic final state interactions leading to non-Abelian energy loss and related modifications to the fragmentation functions [7, 8, 9, 10]. The important question of the global p_T and \sqrt{s} systematics of the nuclear modification factors $R_{BA}(p_T)$ in $p + A$ and $A + A$ reactions has also been addressed [5].

Alternative mechanisms related to hadronic rescattering/absorption, initial state wave-function effects, and coherent nucleon scattering have been suggested [11] as possible explanations of the observed high- p_T hadron deficit. This letter extends the discussion of [5] in light of the upcoming $d + Au$ data and demonstrates how the centrality dependence of the nuclear modification factor can distinguish between contrasting physical pictures. We emphasize the need for comparison between data and theory at moderate and high p_T since vastly different models give comparable results [12] at the level the inclusive dN^{ch}/dy .

The importance of the $d + Au$ measurements at RHIC, however, reaches far beyond testing the validity of the perturbative baseline for jet quenching calculations. In the transverse momentum $2 \leq p_T \leq 10$ GeV and rapidity $-3 \leq y \leq +3$ intervals considered here the measured hadrons retain a memory of the nuclear modifications [13] to the parton distribution functions (PDFs) in the $10^{-3} \leq x \lesssim 1$ range. We find that in the small- x region of the nucleus the multiple elastic scatterings of the incoming partons completely dominate over nuclear shadowing. For large nuclear x -values the EMC effect and the initial state energy loss may lead to moderate (20-30%) suppression relative to the binary collision scaled $p + p$ result over a wide p_T range. The detailed transverse momentum dependence of the nuclear modification ratio may provide valuable complementary information about the gluon anti-shadowing/EMC region, which is not well constrained by data. In fact, the x -dependence in the gluon shadowing function $S_{g/A}(x, Q^2)$ may be significantly weaker than currently anticipated.

II. SCALING OF HADRON SPECTRA IN $d + Au$ REACTIONS

The Cronin effect [14] is defined as the deviation of the total invariant hadron cross section in $p + A$ reactions from the binary collision scaled $p + p$ result. For the more general case of $B + A$ reactions the scaling factor is given by $B \cdot A$. The original parametrization of dynamical nuclear effects via the Cronin power $\alpha(p_T)$ relates to the nuclear modification ratio $R_{BA}(p_T)$ as follows: $R_{pA}(p_T) = A^{\alpha(p_T)-1}$. The same relation (without additional factors of 2 since the partons from the nucleus do not scatter significantly on the deuteron) can also be used to extract a total inclusive $\alpha_{dAu}(p_T)$ and a centrality dependent $\alpha_{dAu}(p_T, b)$ from

$$R_{dAu}(p_T) = \begin{cases} \frac{d\sigma^{dAu}}{dyd^2\mathbf{p}_T} / \frac{A_d \cdot A_{Au} d\sigma^{pp}}{dyd^2\mathbf{p}_T}, & \text{total invariant cross section, } d + Au \\ \frac{dN^{dAu}(b)}{dyd^2\mathbf{p}_T} / \frac{T_{dAu}(b) d\sigma^{pp}}{dyd^2\mathbf{p}_T}, & \text{about impact parameter } b, \text{ } d + Au \end{cases}. \quad (1)$$

In Eq.(1) $T_{dAu}(b) = \int d^2\mathbf{r} T_d(\mathbf{r})T_{Au}(\mathbf{b} - \mathbf{r})$ in terms of the nuclear thickness functions $T_A(b) = \int dz \rho_A(b, z)$ and the scaling factors are computed according to the Glauber model [15]. It is important to note that both enhancement ($p_T \gtrsim 1.5 - 2$ GeV) and suppression ($p_T \lesssim 1 - 1.5$ GeV) are an integral part of the Cronin effect. Experimentally [14], at $p_T = 0.77$ GeV $\alpha(p_T)$ is below one, leading to a factor ~ 2 suppression. However, the deviation of $\alpha(p_T)$ from unity is reduced with increasing \sqrt{s} and decreasing $x_T = 2p_T/\sqrt{s}$ - a trend exactly opposite to the expectation from strong shadowing and/or gluon saturation. The p_T positions of the Cronin peak $R_{pA} \text{ max}$ and intercept $R_{pA} = 1$ are also stable, i.e. they are strongly x_T -dependent.

The lowest order pQCD differential cross section for inclusive $A + B \rightarrow h + X$ production that enters Eq.(1) is given by [5, 16]

$$\left. \begin{aligned} & \frac{1}{A_d \cdot A_{Au}} \frac{d\sigma^{dAu}}{dyd^2\mathbf{p}_T} \\ & \frac{1}{T_{dAu}(b)} \frac{dN^{dAu}(b)}{dyd^2\mathbf{p}_T} \end{aligned} \right\} = K \cdot \sum_{abcd} \int dx_a dx_b \int d^2\mathbf{k}_a d^2\mathbf{k}_b \otimes g(\mathbf{k}_a)g(\mathbf{k}_b) \otimes S_d(x_a, Q_a^2)S_{Au}(x_b, Q_b^2) \\ \otimes f_{a/d}(x_a, Q_a^2)f_{b/Au}(x_b, Q_b^2) \otimes \frac{d\sigma^{ab \rightarrow cd}}{d\hat{t}} \otimes \frac{D_{h/c}(z_c, Q_c^2)}{\pi z_c}, \quad (2)$$

where we have used the same sets of lowest order (LO) PDFs, fragmentation functions (FFs), and shadowing functions [17] as in [5]. In Eq.(2) the renormalization, factorization, and fragmentation scales are chosen to be $\mu = Q_{a,b} = Q_c = p_T$.

The the k_T -broadening function in (2) approximates generalized parton distributions:

$$f_{a/p}(\mathbf{k}_T; x_a, Q_a^2) \simeq g(\mathbf{k}_T) \otimes f_{a/p}(x_a, Q_a^2), \quad g(\mathbf{k}_T) = \frac{1}{\pi \langle \mathbf{k}_T^2 \rangle_{pp}} \exp \left(-\frac{\mathbf{k}_T^2}{\langle \mathbf{k}_T^2 \rangle_{pp}} \right) . \quad (3)$$

For illustration we include a discussion of parton broadening relative to the axis of propagation in the framework of the leading double log approximation (LDLA). The \mathbf{k}_T probability distribution resulting from vacuum radiation is given by [18]

$$\frac{1}{\sigma_0} \frac{d\sigma}{d\mathbf{k}_T^2} \Big|_{LDLA} = -2 \frac{C_R \alpha_s}{2\pi} \frac{1}{\mathbf{k}_T^2} \log \frac{\mathbf{k}_T^2}{Q^2} \exp \left(-\frac{C_R \alpha_s}{2\pi} \log^2 \frac{\mathbf{k}_T^2}{Q^2} \right) \quad (4)$$

with mean broadening $\langle \mathbf{k}_T^2 \rangle_{pp} = C_R \alpha_s / \pi (1 + \mathcal{O}(\alpha_s)) Q^2$. $C_R = \{C_F, C_A\}$ is the SU(3) Casimir in the corresponding fundamental or adjoint representation. Despite the strong momentum ordering approximation [18], which gives an unrealistic null probability for retaining the original jet direction, Eq.(4) qualitatively describes many the jet physics features. For example, with $\frac{1}{2}\theta_m = \sqrt{\langle \mathbf{k}_T^2 \rangle_{pp}/Q^2} \simeq \sqrt{C_R \alpha_s / \pi}$ being the estimate for the half-width of the jet cone a slow logarithmic narrowing with E_T is predicted. Similarly, to lowest order the cone of a gluon initiated jet is found to be 50% wider ($\sqrt{C_A/C_F}$) than the cone of a quark jet.

\sqrt{s} [GeV]	19.4	27.4	38.8	200
$F_q^h(\sqrt{s})$	0.220	0.150	0.096	0.015
$\langle \mathbf{k}_T^2 \rangle_{pp}$ [GeV]	1.700	1.775	1.835	1.920
$\Delta(\sqrt{s})$	0.958	1.000	1.034	1.082

TABLE I: The fractional contribution of valance quark hard scattering to hadron production at $y = 0$, $\bar{Q} = p_T \simeq 2.5$ GeV versus \sqrt{s} . The vacuum radiation induced parton broadening computed from Eq.(5) and its variation $\Delta(\sqrt{s})$ relative to the $\sqrt{s} = 27.4$ GeV reference are also shown.

In this letter we go beyond the \sqrt{s} -independent description of the radiative and elastic broadening and take into account the initial parton subprocesses for produced hadrons. An increased contribution of hard gluon scattering results in an enhanced

$$\langle \mathbf{k}_T^2 \rangle_{pp} = (C_F F_q^h(\sqrt{s}, \bar{Q}) + C_A F_g^h(\sqrt{s}, \bar{Q})) C^2 . \quad (5)$$

In Eq.(5) $F_q^h(\sqrt{s}, \bar{Q})$, $F_g^h(\sqrt{s}, \bar{Q}) = 1 - F_q^h(\sqrt{s}, \bar{Q})$ are the fractions of hadrons coming from the hard scattering of valance quarks and gluons/sea quarks. With sea quarks we associate

the Casimir of their gluon parent ($g \rightarrow \bar{q}q$). For hadrons with $p_T = \bar{Q} \simeq 2-3$ GeV where the k_T -smearing is reflected, the fraction coming from valence quarks is computed from collinear factorized pQCD and given in Table I. The corresponding $\langle \mathbf{k}_T^2 \rangle_{pp}$ is found from Eq.(5) where $C^2 = 0.646$ GeV² has been fixed through comparison to the $\sqrt{s} = 27.4$ GeV data [14] on $\frac{1}{2}(\pi^+ + \pi^-)$ production in $p + p$. $\Delta(\sqrt{s}) = \langle \mathbf{k}_T^2(\sqrt{s}) \rangle_{pp} / \langle \mathbf{k}_T^2(27.4 \text{ GeV}) \rangle_{pp}$ in Table I directly reflects the variation with \sqrt{s} of the effective mean color charge of \sim few GeV projectile partons relative to the $\sqrt{s} = 27.4$ GeV case.

We have checked that the energy and transverse momentum dependence of inclusive hadron production cross sections is well described with the computed values of $\langle \mathbf{k}_T^2 \rangle_{pp}$ which exhibit a small $< 10\%$ variation about $\langle \mathbf{k}_T^2 \rangle_{pp} = 1.8$ GeV² used in [5].

III. IMPLEMENTATION OF INITIAL STATE ENERGY LOSS

While there are indications that the effect of initial state gluon bremsstrahlung may be small [19] the elastic energy loss of propagating hard probes in cold nuclear matter has not been considered before. Discussion of QCD scattering in nuclear targets can be found in [20]. In both frameworks of the Qiu-Sterman approach and the Gyulassy-Levai-Vitev reaction operator approach the *longitudinal* correction that corresponds to the transverse momentum broadening can be expressed through the momentum shift operators $e^{-q_{i\parallel} \partial_{k_{i\parallel}}}$. The initial parton flux $d^3 N^i(k_{\parallel}, \mathbf{k}_{\perp})$ flux is propagated to the hard collision vertex according to [21]:

$$\frac{d^3 N^f(k_{\parallel}, \mathbf{k}_{\perp})}{dk_{\parallel} d^2 \mathbf{k}_{\perp}} = \sum_{n=0}^{\infty} \frac{\chi^n}{n!} \int \prod_{i=1}^n d^2 \mathbf{q}_{i\perp} \left[\frac{1}{\sigma_{el}} \frac{d\sigma_{el}}{d^2 \mathbf{q}_{i\perp}} \left(e^{-\mathbf{q}_{i\perp} \cdot \vec{\nabla}_{\mathbf{k}_{\perp}}} \otimes e^{-q_{i\parallel} \partial_{k_{i\parallel}}} - 1 \right) \right] \times \frac{d^3 N^i(k_{\parallel}, \mathbf{k}_{\perp})}{dk_{\parallel} d^2 \mathbf{k}_{\perp}} . \quad (6)$$

From the twist expansion point of view the series Eq.(6) includes the dominant part of all-twist $T = 2 + 2n$ contributions $\langle q(2n FF)q \rangle, \langle F(2n FF)F \rangle$. Explicit resummation technique for (6) was first given in [20]. The interpretation of our result is simple: it folds the Poisson distribution of multiple elastic scatterings with mean opacity $\chi = \langle L \rangle / \lambda = \bar{n}$, which depends on the quark/gluon composition of the target and the projectile, with the probability for transverse deflection per hit given by the normalized elastic scattering cross section $(1/\sigma_{el}) d\sigma_{el}/d^2 \mathbf{q}_{i\perp}$. For proton-nucleus collisions using a sharp sphere approxima-

tion ($T_A(b) = 3A\sqrt{R_A^2 - b^2}/(2\pi R_A^3)$) and assuming equal scattering probability along the incident parton trajectory

$$\langle L \rangle = \frac{\int d^2\mathbf{b} \sqrt{R_A^2 - b^2} T_A(b)}{\int d^2\mathbf{b} T_A(b)} = \frac{3}{4} R_A \quad , \quad (7)$$

where we take $R_A = 1.2A^{1/3}$ fm for the nuclear radius. One of the important consequences [21] of Eq.(6) is the longitudinal momentum backward shift

$$-\Delta k_{\parallel} = \mu^2 \chi \xi \frac{1}{2k_{\parallel}} \quad (8)$$

that couples to the mean k_{\perp} -broadening $\langle \Delta k_{\perp}^2 \rangle_{pA} = \mu^2 \chi \xi$. For the Gaussian approximation to multiple elastic scatterings, $\xi = \text{const.} = \mathcal{O}(1)$. Beyond this analytically convenient ansatz the power law tails of the distribution of the scattered partons, resulting from harder fluctuations along the projectile path, lead to a logarithmic enhancement of the mean k_{\perp} -broadening. This result is the analogue of the corrections to the Moliere multiple collision series in QED. We use $\xi = \ln(1 + \tilde{c}p_{\perp}^2)$ as in Ref. [5] with $\tilde{c} \simeq 0.14 \text{ GeV}^{-2}$.

To implement *initial state* elastic and radiative energy loss we focus on the large $Q^2 \simeq p_T^2$ partonic subprocess $ab \rightarrow cd$, k_a, k_b being the initial momenta involved in the hard part $d\sigma^{ab \rightarrow cd}/dt$ of Eq.(2). If a, b have lost fractions ϵ_{α} , $\alpha = a, b$ of their longitudinal momenta according to a probability distributions $P_{\alpha}(\epsilon)$, at asymptotic $t = -\infty$

$$\tilde{k}_{\alpha} = \frac{1}{1 - \epsilon_{\alpha}} k_{\alpha} \quad , \quad f_{\alpha/p}(x_{\alpha}, Q^2) \rightarrow \int d\epsilon_{\alpha} P_{\alpha}(\epsilon_{\alpha}) f_{\alpha/p} \left(\tilde{x}_{\alpha} = \frac{x}{1 - \epsilon_{\alpha}}, Q^2 \right) \theta(\tilde{x}_{\alpha} \leq 1) \quad . \quad (9)$$

Eq.(9) provides a simple modification to the factorized pQCD hadron production formalism. For bremsstrahlung processes $P_{\alpha}(\epsilon)$ are sensitive to multiple gluon emission [9]. For the simpler case of mean energy loss $P(\epsilon) = \delta(\epsilon - \langle \Delta k_0 \rangle / k_0)$. More specifically, for the small elastic longitudinal shift that we consider here

$$P_{\alpha}(\epsilon) = \delta \left(\epsilon - \frac{\mu^2 \chi_{\alpha} \xi}{2k_{\alpha}^2} \right) \quad , \quad f_{\alpha/p}(x_{\alpha}, Q^2) \rightarrow f_{\alpha/p} \left(x_{\alpha} + \frac{\mu^2 \chi_{\alpha} \xi}{x_{\alpha}} \frac{2}{s}, Q^2 \right) \theta(\tilde{x}_{\alpha} \leq 1) \quad . \quad (10)$$

The observable effect of Eqs.(9,10) can be very different for valence quarks, sea quarks, and gluons due to the different x -dependence of the PDFs.

Two fits to the $\sqrt{s} = 27.4, 38.8 \text{ GeV}$ $p+W/p+Be$ data are given in Fig. 1. In the first case we use the EKS'98 shadowing function $S_{\alpha/A}(x_{\alpha}, Q^2)$ to model the antishadowing/EMC modification of the nuclear target. The changing quark/gluon projectile composition, reflected

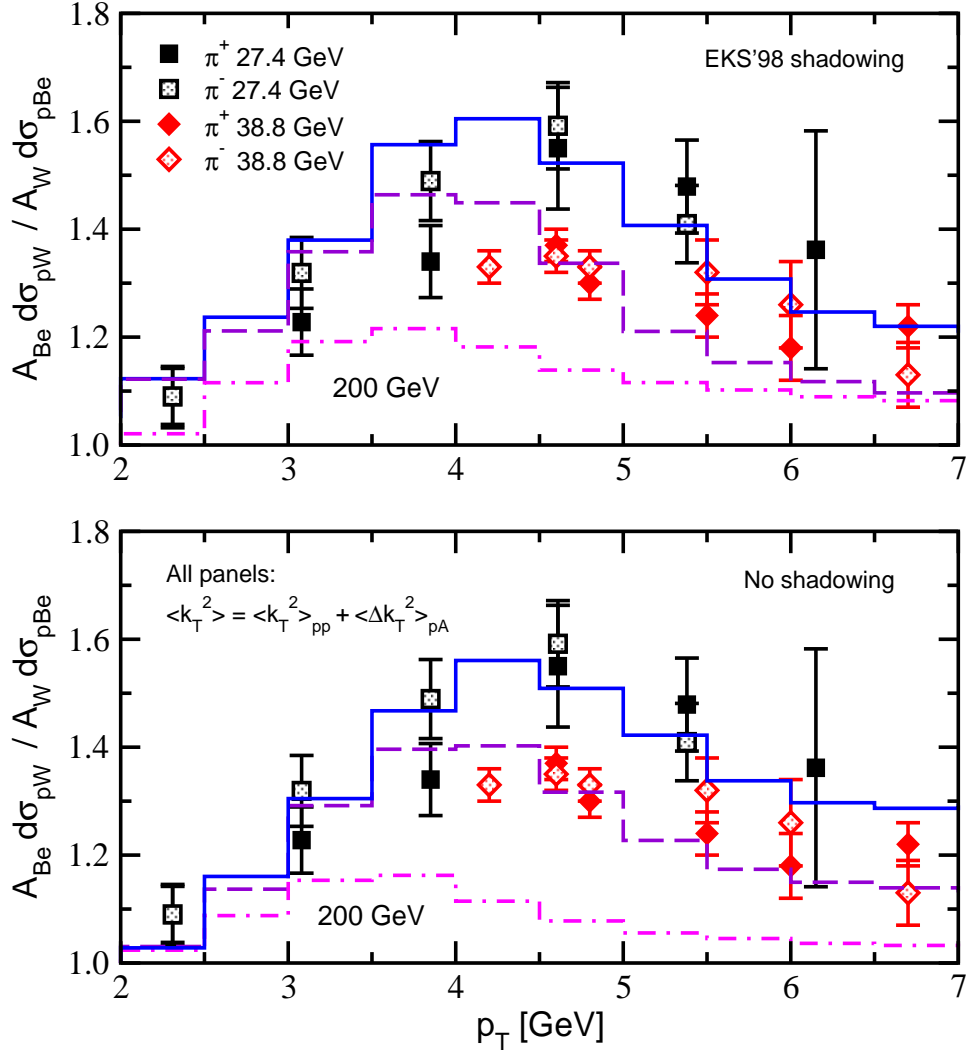


FIG. 1: The ratio of A -scaled $p + W/p + Be$ data on π^+, π^- production at $\sqrt{s} = 27.4, 38.8$ GeV from [14]. Calculations are for $\frac{1}{2}(\pi^+ + \pi^-)$: top/bottom panel include/do not include anti-shadowing/EMC effect as described in the text. The anticipated $\sqrt{s} = 200$ GeV $p + W/p + Be$ ratio is shown to illustrate the energy dependence of the Cronin effect.

in its \sqrt{s} -dependent average color charge, enters the opacity through the elastic scattering cross section:

$$\chi(\sqrt{s}) = \sigma_{el} \rho \langle L \rangle \propto (C_F F_q^h(\sqrt{s}, \bar{Q}) + C_A F_g^h(\sqrt{s}, \bar{Q})) \bar{C}_T, \quad (11)$$

i.e. in a way analogous to Eq.(5). In Eq.(11) \bar{C}_T is the mean color charge of the target. The variation of the opacity with the center of mass energy can thus be inferred from Table I and is given by $\chi(\sqrt{s}) = \Delta(\sqrt{s}) \cdot \chi(27.4 \text{ GeV})$ for fixed \bar{C}_T . While quark antishadowing/EMC

effect are constrained by data, the modifications to the gluon PDFs are quite uncertain. In the second calculation we do not include nuclear shadowing. Instead, in Eq.(11) we also take a changing average color charge for the target: $C_T(\sqrt{s}) = (C_F F_q^h(\sqrt{s}, \bar{Q}) + C_A F_g^h(\sqrt{s}, \bar{Q}))$. In this case the variation of the effective opacity with \sqrt{s} is given by $\chi(\sqrt{s}) = \Delta^2(\sqrt{s}) \cdot \chi(27.4 \text{ GeV})$. Both calculations include initial state mean elastic energy loss. With the definition of $\langle L \rangle$ given in Eq.(7) the transport coefficients of cold nuclear matter are fixed to $\mu^2/\lambda_q \approx 0.06 \text{ GeV}^2/\text{fm}$, $\mu^2/\lambda_g = (C_A/C_F) \mu^2/\lambda_q \approx 0.14 \text{ GeV}^2/\text{fm}$. The modest $\sim 20\%$ increase relative to previous estimates ($\mu^2/\lambda_q \simeq 0.05 \text{ GeV}^2/\text{fm}$ [5]) compensates for the longitudinal backward momentum shift, Eq.(8), and provides comparable reproduction of existing low energy $p + A$ results. This can be seen by comparing the top panel of Fig. 1 to Fig. 1 from Ref. [5]. The bottom panel of Fig. 1 seems to show better agreement between data and theory in terms of improved reproduction of the Cronin peak and separation of the nuclear modification ratios versus \sqrt{s} at high p_T . We continue to explore both possibilities but the calculations without strong antishadowing/EMC effect are also expected to give better results at RHIC energies.

The systematic reduction of the Cronin enhancement/suppression with increasing \sqrt{s} has its natural explanation in the picture of multiple elastic scattering on a nuclear target [20] (see Fig. 1). With the opacity χ changing only slightly with \sqrt{s} the dominant effect becomes the significant hardening of the hadronic spectra as predicted by perturbative QCD. This reduces the observable consequences of otherwise identical transverse momentum kicks.

We have also checked that the flavor dependence of the Cronin effect - the larger enhancement/suppression for kaons (and also protons) - cannot be reproduced within the accuracy of the calculation. Studies have so far been focused on the baryon enhancement puzzle [22] but the results are inconclusive. We note that improved perturbative techniques are necessary to address the Cronin effect for massive hadrons and extend the calculations to the $p_T \lesssim 2 \text{ GeV}$ region.

IV. IMPACT PARAMETER AND RAPIDITY DEPENDENCE OF THE CRONIN EFFECT

The $\sqrt{s} = 200 \text{ GeV}$ results for the Cronin effect in $d + Au$ reactions at midrapidity are shown in Fig. 2. At $y = 0$ for the corresponding $2 \times 10^{-2} \leq x_T \leq 10^{-1}$ values the shadowing

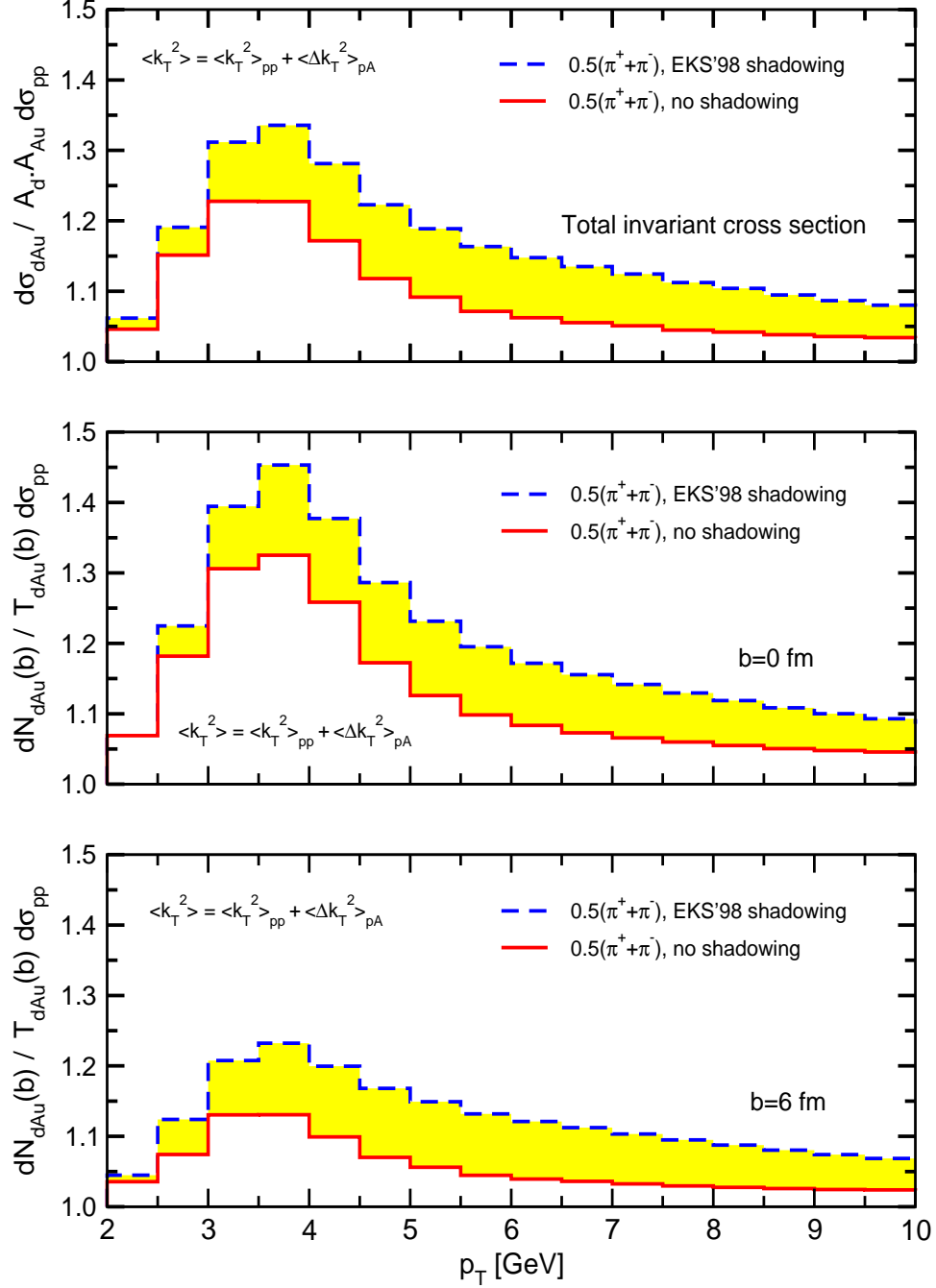


FIG. 2: The Cronin effect, represented by the nuclear modification ratio $R_{dAu}(p_T)$, for $\frac{1}{2}(\pi^+ + \pi^-)$ is shown for the total invariant cross section and impact parameters $b = 0, 6$ fm.

region of $S_{a/A}(x, Q^2)$ is never reached. However, the relative contribution of antishadowing is seen to be large for $p_T \geq 3$ GeV. We find that without significant x -dependent modification of the nuclear target (i.e. the case that gives better agreement with existing data from Fig. 1) the Cronin enhancement reaches 1.2 with peak position ($R_{dAu \text{ max}}$) in the $p_T \simeq 3 - 4$ GeV

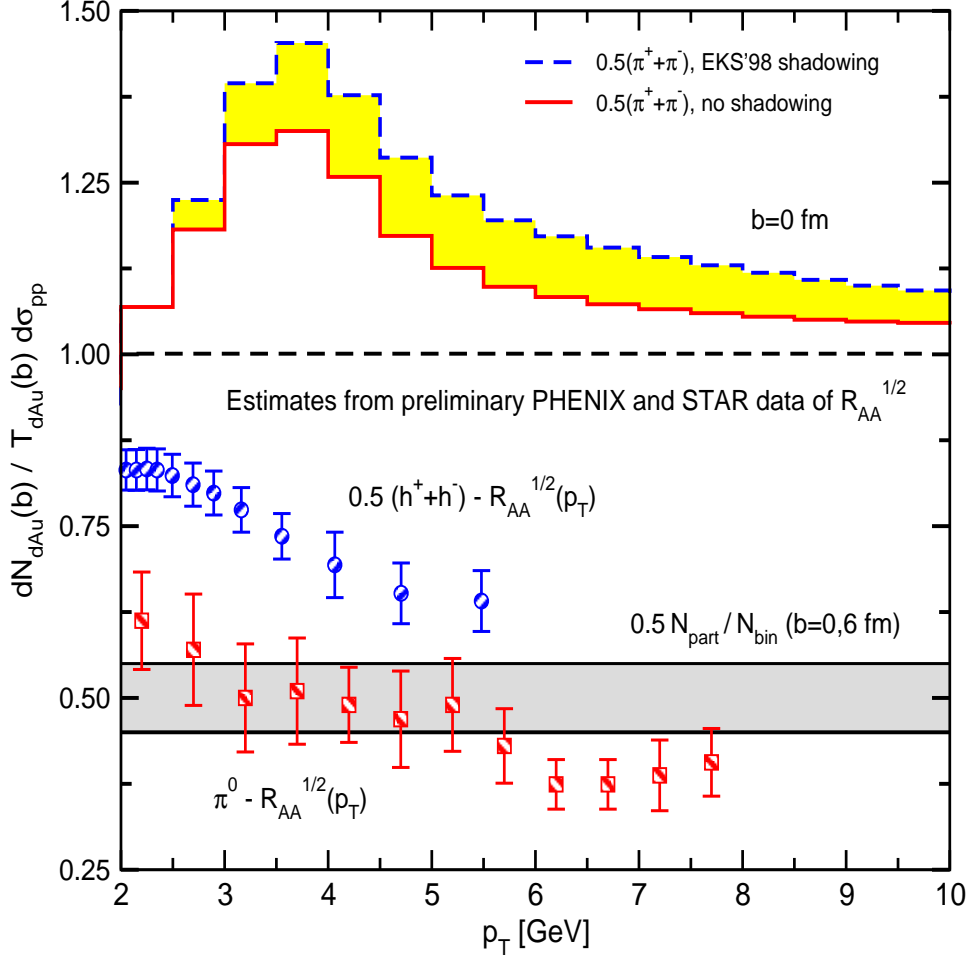


FIG. 3: Illustration of the difference between the computed small $\sim 5 - 10\%$ Cronin enhancement at $p_T \geq 5$ GeV in central reactions and the argued [11] factor of 30 – 50% suppression. The estimated $\sqrt{R_{AA}(p_T)}$ for $\frac{1}{2}(h^+ + h^-)$ and π^0 from preliminary STAR and PHENIX data [1] and the $N_{part}/2$ scaling for $b = 0, 6$ fm are shown.

range, a 30% drop relative to the strong gluon antishadowing scenario. In going from central ($b = 0$ fm) to peripheral ($b = 6$ fm) reactions the magnitude of the Cronin effect is reduced by a factor ~ 2.5 . The main uncertainty in computing $R_{dA}(p_T)$ for peripheral reactions comes from the large deuteron radius, leading to a distribution in impact parameter of its partonic constituents. The corresponding spread in opacity $\chi = \sqrt{R_A^2 - b^2}/\lambda$ grows with increasing b and using the average value $\chi(b)$ in Eqs.(6,8) may not be a good approximation.

Midrapidity measurements accessible to all experiments, especially for central reactions, are the prime candidate that can distinguish between different hadron production scenarios. Glauber model calculations [15] that account for the large deuteron radius show a factor ~ 2

difference between N_{bin} and $N_{part}/2$ (not $N_{part}!$), the two possible scalings relative to $p + p$, over a wide range of impact parameters. Participant scaling at moderate and high p_T (up to $p_T = 8 - 10$ GeV as discussed in [11]) will correspond to $R_{dAu}(p_T) \simeq 0.5$ as shown in Fig. 3. The gluon saturation model suggests $R_{dAu}(p_T) = \sqrt{R_{AuAu}(p_T)}$, i.e. it will in fact lead to the same conclusion since the suppression in $Au + Au$ reactions is 3-5 fold. This is demonstrated in Fig. 3 through the estimated $\sqrt{R_{AuAu}(p_T)}$ for inclusive charged hadrons and neutral pions from preliminary STAR and PHENIX data [1]. We emphasize that the p_T dependence of the nuclear modification ratio in $d + Au$ is different as well. Final state hadron absorption mechanisms [11] are also expected to result in suppression in $d + Au$, albeit smaller and difficult to quantify analytically. In contrast, the calculations in Figs. 2 and 3 show small enhancement in the specified p_T range even with initial state elastic energy loss. Predictions that have quantitatively addressed the $y = 0$, $p_T \geq 2$ GeV Cronin effect at RHIC from the standpoint of perturbative QCD and multiple elastic scatterings give similar results [5, 16]. Experimental measurements in $d + Au$ will enable a critical test to differentiate between competing interpretations of $Au + Au$ data.

Fig. 4 shows the predicted Cronin effect at forward ($y = +3$) and backward ($y = -3$) rapidities near the edge of BRAHMS acceptance. In the following calculations the direction of the deuteron beam is chosen to be positive. At forward rapidity, which probes the small- x region of the nucleus, the effect of shadowing is very small. Similarly, turning off elastic energy loss does not significantly change the shape and magnitude of $R_{dAu}(p_T)$. Relative to $y = 0$, both the peak and intercept ($R_{dAu} = 1$) positions are shifted to slightly higher transverse momenta. The most distinct prediction at $y = +3$ is the significantly flatter Cronin enhancement region that extends to high p_T . At forward/backward rapidities hadron spectra are much steeper than at $y = 0$. This explains the markedly broader range where the effect of transverse momentum kicks is observed.

At backward $y = -3$ rapidity, shown at the bottom panel of Fig. 4, there is no Cronin enhancement since the partons from the nucleus do not scatter multiply on the deuteron. However, in the p_T range shown data probes the large $x \gtrsim 0.4$ nuclear modification $S_{a/A}(x, Q^2)$ and may provide complementary information about the EMC effect. The backward rapidity region is also more sensitive to initial state energy loss. Switching it off changes $R_{dAu}(p_T)$ from moderate $\sim 25\%$ suppression to an almost perfect binary collision scaling ($R_{dAu}(p_T) \simeq 1$) for $p_T \geq 3$ GeV.

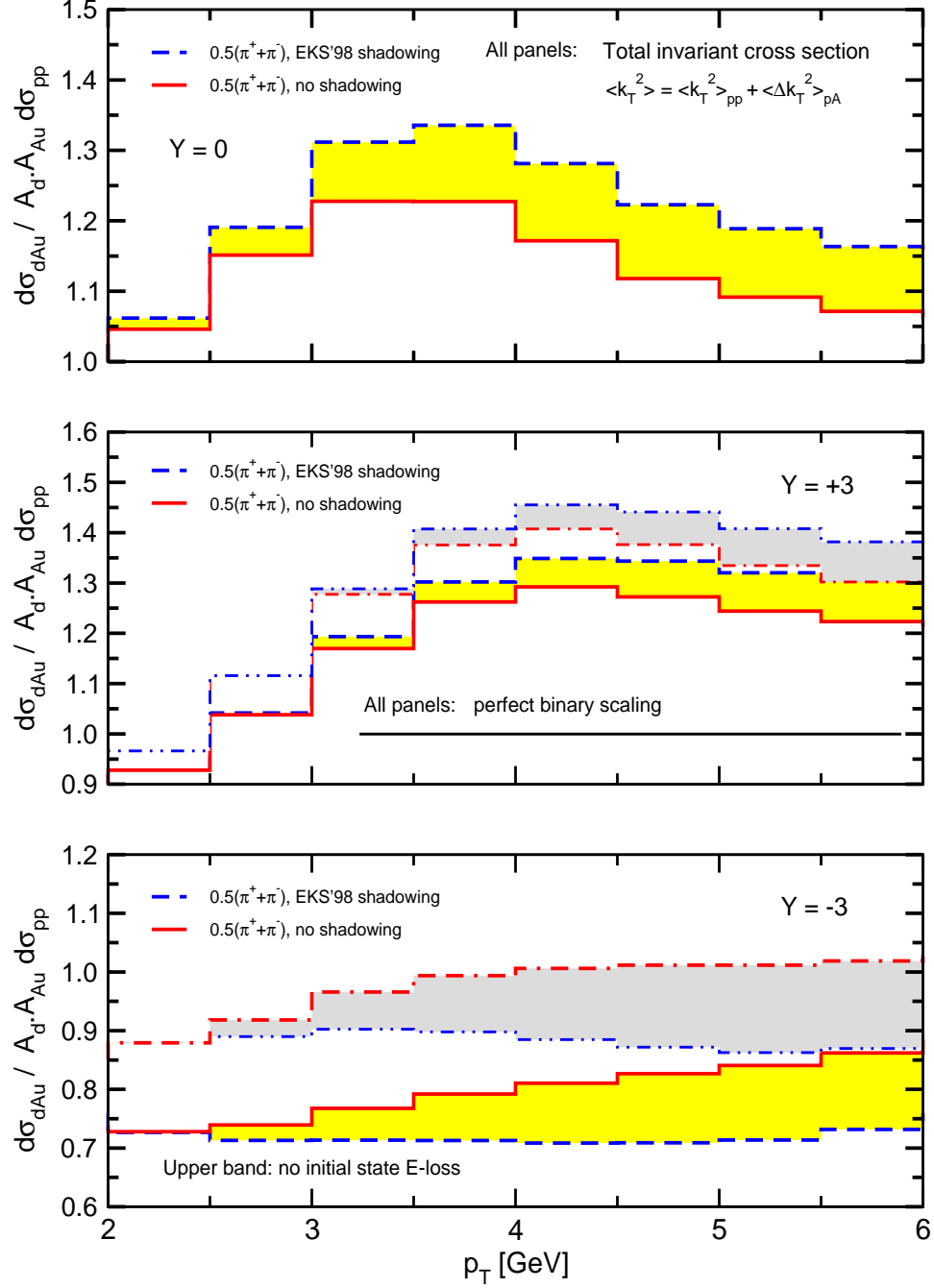


FIG. 4: Rapidity dependence of the Cronin effect in $d + Au$ reactions at $\sqrt{s_{NN}} = 200$ GeV with and without antishadowing/EMC effect. The result of switching off elastic energy loss is also shown via the upper bands for $y = \pm 3$.

V. CONCLUSIONS

In this letter we have derived a technique of incorporating initial state parton energy loss in perturbative calculations. Midrapidity moderate- and high- p_T hadron spectra show little or no sensitivity to this effect since the longitudinal momentum backward shifts can be compensated by a small increase in the estimated cold nuclear transport coefficients to obtain an equally good description of existing $p + A$ data. Detecting initial state energy loss may be easier in the small- x region of the deuteron where the steepening of the parton distribution functions would tend to amplify the effect.

In this letter we have given predictions for the centrality and rapidity dependence, see Figs. 2 and 4, of the moderate and high transverse momentum ($p_T \geq 2$ GeV) Cronin effect in $d + Au$ reactions at RHIC. They follow the systematic approach to the computation of the nuclear modification factors outlined in Ref. [5]. At midrapidity we find a small $\sim 20 - 30\%$ Cronin enhancement that decreases in going from central to peripheral reactions and at high p_T . Forward and backward ($y = \pm 3$) rapidity regions are predicted to have markedly different $R_{dA}(p_T)$. Upcoming central $d + Au$ data will provide a decisive test to distinguish between suppression and enhancement dynamical models [5, 11, 16], see Fig. 3, of initial state effects in nuclear collisions.

Acknowledgments

Many illuminating discussions with M. Gyulassy, J.W. Qiu, and J.P. Vary are gratefully acknowledged. I would like to thank J. Klay and D. d'Enterria for clarifying comments on the preliminary STAR and PHENIX data. This work is supported by the United States Department of Energy under Grant No. DE-FG02-87ER40371.

-
- [1] K. Adcox *et al.*, Phys. Rev. Lett. **88**, 022301 (2002); C. Adler *et al.*, Phys. Rev. Lett. **89**, 202301 (2002); J. L. Klay, arXiv:nucl-ex/0210026; S. Mioduszewski, arXiv:nucl-ex/0210021; J. Jia, arXiv:nucl-ex/0209029; D. d'Enterria, arXiv:hep-ex/0209051; C. Roland *et al.*, arXiv:hep-ex/0212006.

- [2] P. Levai, G. Papp, G. Fai, M. Gyulassy, G. G. Barnafoldi, I. Vitev and Y. Zhang, Nucl. Phys. A **698**, 631 (2002).
- [3] C. Adler *et al.*, arXiv:nucl-ex/0206006; K. Filimonov, arXiv:nucl-ex/0210027; N. N. Ajitanand, arXiv:nucl-ex/0210007.
- [4] C. Adler *et al.*, arXiv:nucl-ex/0210033; D. Hardtke, arXiv:nucl-ex/0212004; M. Chiu, arXiv:nucl-ex/0211008.
- [5] I. Vitev and M. Gyulassy, Phys. Rev. Lett. **89**, 252301 (2002).
- [6] T. Hirano and Y. Nara, arXiv:nucl-th/0301042; S. Y. Jeon, J. Jalilian-Marian and I. Sarcevic, arXiv:nucl-th/0208012; F. Arleo, JHEP **0211**, 044 (2002); E. Wang and X. N. Wang, Phys. Rev. Lett. **89**, 162301 (2002); M. Gyulassy, I. Vitev and X. N. Wang, Phys. Rev. Lett. **86**, 2537 (2001).
- [7] B.G. Zakharov, JETP Lett. **63**, 952 (1996); R. Baier *et al.*, Nucl. Phys. B **484**, 265 (1997); U.A. Wiedemann, Nucl. Phys. B **588**, 303 (2000).
- [8] M. Gyulassy, P. Levai and I. Vitev, Phys. Rev. Lett. **85**, 5535 (2000); M. Gyulassy, P. Levai and I. Vitev, Nucl. Phys. B **594**, 371 (2001).
- [9] M. Gyulassy, P. Levai, and I. Vitev, Phys. Lett. B **538**, 282 (2002); R. Baier, Y. L. Dokshitzer, A. H. Mueller and D. Schiff, JHEP **0109**, 033 (2001).
- [10] X. N. Wang and X. F. Guo, Nucl. Phys. A **696**, 788 (2001); C. A. Salgado and U. A. Wiedemann, Phys. Rev. Lett. **89**, 092303 (2002); J. A. Osborne, E. Wang and X. N. Wang, arXiv:hep-ph/0212131.
- [11] K. Gallmeister, C. Greiner and Z. Xu, arXiv:hep-ph/0212295; D. Kharzeev, E. Levin and L. McLerran, arXiv:hep-ph/021033; R. Lietava, J. Pisut, N. Pisutova and B. Tomasik, arXiv:nucl-th/0301052.
- [12] Z. W. Lin and C. M. Ko, arXiv:nucl-th/0301025; D. Kharzeev, E. Levin and M. Nardi, arXiv:hep-ph/0212316; HIJING 1.37 simulation, X.-N. Wang and M. Gyulassy, Phys. Rev. Lett. **68**, 1480 (1992).
- [13] M. Arneodo, Phys. Rept. **240**, 301 (1994); A. H. Mueller and J. W. Qiu, Nucl. Phys. B **268**, 427 (1986); S. J. Brodsky and H. J. Lu, Phys. Rev. Lett. **64**, 1342 (1990); H. J. Pirner and J. P. Vary, Phys. Rev. Lett. **46**, 1376 (1981).
- [14] J. Cronin *et al.*, Phys. Rev. D **11**, 3105 (1975); D. Antreasyan *et al.*, Phys. Rev. D **19**, 764 (1979); P. B. Straub *et al.*, Phys. Rev. Lett. **68**, 452 (1992).

- [15] R. J. Glauber and G. Matthiae, Nucl. Phys. B **21**, 135 (1970).
- [16] A. Accardi, arXiv:hep-ph/0212148; Y. Zhang, G. Fai, G. Papp, G. G. Barnafoldi and P. Levai, Phys. Rev. C **65**, 034903 (2002); X.-N. Wang, Phys. Rev. C **61**, 064910 (2000); B. Z. Kopeliovich, J. Nemchik, A. Schafer and A. V. Tarasov, Phys. Rev. Lett. **88**, 232303 (2002)
- [17] M. Glück, E. Reya, and A. Vogt, Eur. Phys. J. **C5**, 461 (1998); J. Binnewies, B.A. Kniehl, and G. Kramer, Z. Phys. C **65**, 471 (1995); K.J. Eskola, V.J. Kolhinen, and C.A. Salgado, Eur. Phys. J. C **9**, 61 (1999).
- [18] R. Field, *Applications of Perturbative QCD*, Addison-Wesley Publishing Co., 1989; V. V. Sudakov, Sov. Phys. JETP **3** (1956) 65 [Zh. Eksp. Teor. Fiz. **30** (1956) 87].
- [19] F. Arleo, Phys. Lett. B **532**, 231 (2002); R. Baier, arXiv:hep-ph/0209038.
- [20] J. W. Qiu and G. Sterman, arXiv:hep-ph/0111002; M. Gyulassy, P. Levai and I. Vitev, Phys. Rev. D **66**, 014005 (2002).
- [21] I. Vitev and J.W. Qiu, work in preparation.
- [22] I. Vitev and M. Gyulassy, Phys. Rev. C **65**, 041902 (2002); X. F. Zhang, G. Fai and P. Levai, Phys. Rev. Lett. **89**, 272301 (2002); R. C. Hwa and C. B. Yang, arXiv:nucl-th/0211010.